Received: 6 October 2020 | Accepted: 27 October 2020

DOI: 10.1111/1365-2745.13552

Journal of Ecology | BRITISH ECOLOGICAL SOCIETY

RECONCILING RESILIENCE ACROSS ECOLOGICAL SYSTEMS, SPECIES AND SUBDISCIPLINES

Research Article

Stress gradients interact with disturbance to reveal alternative states in salt marsh: Multivariate resilience at the landscape scale

Scott F. Jones[1,2] | Camille L. Stagg[3] | Erik S. Yando[2,4] | W. Ryan James[2] | Kevin J. Buffington[1] | Mark W. Hester[2]

[1]U.S. Geological Survey, Western Ecological Research Center, Davis, CA, USA

[2]Department of Biology, University of Louisiana at Lafayette, Lafayette, LA, USA

[3]U.S. Geological Survey, Wetland and Aquatic Research Center, Lafayette, LA, USA

[4]Department of Biological Sciences, Old Dominion University, Norfolk, VA, USA

Correspondence
Scott F. Jones
Email: sfjones@usgs.gov

Funding information
U.S. Geological Survey South Central Climate Adaptation Science Center; Center for Ecology and Environmental Technology, University of Louisiana at Lafayette; Society of Wetland Scientists

Handling Editor: Christine Angelini

Abstract

1. Stress gradients influence many ecosystem processes and properties, including ecosystem recovery from and resistance to disturbance. While recent analytical approaches have advanced multivariate metrics of ecosystem resilience that allow quantification of conceptual resilience models and identification of thresholds of state change, these approaches are not often translated to landscape scales.
2. Using natural and restored salt marshes in Louisiana, USA, we quantified plant community recovery and resistance metrics along flooding stress gradients. *n*-dimensional hypervolumes of plant community biomass and structure were simulated using field data collected from disturbance-recovery experiments. The relationships between multivariate resilience metrics and flooding stress gradients were then mapped at community- and landscape-relevant scales by scaling with airborne-derived data across the region.
3. Greater pre-disturbance abiotic stress decreased live below-ground, but not above-ground, biomass, and ultimately led to lower post-disturbance total recovery, recovery rates and resistance of plant communities. Vegetated plots flooded >52% of the time transitioned to an alternative, unvegetated state after disturbance. Mapping revealed differences in spatial patterns of resilience—highlighting low, interior marsh edges as especially vulnerable to the combination of chronic flooding stress and acute disturbance. At the landscape scale, approximately half of the area (48%) is vulnerable to state change after pulse disturbances.
4. *Synthesis*. Ultimately, we quantify the ball-and-cup conceptual model for a salt marsh ecosystem and its alternative state, mudflat. We find that increasing abiotic stress due to climate change diminishes ecosystem resilience, but the interaction with common episodic disturbances is necessary to reveal transitions to alternative states and quantify state change thresholds. Quantifying and mapping resilience and where alternative states may exist in this fashion improves ecologists' ability to investigate the mechanisms of stress gradient control on emergent ecosystem properties while providing spatially explicit resources for managing ecosystems according to their projected resilience.

KEYWORDS
alternative states, coastal wetlands, disturbances, *n*-dimensional hypervolumes, recovery, resilience, resistance, stress gradients

1 | INTRODUCTION

Ecosystem structure and function are controlled by a variety of abiotic and biotic drivers that interact across spatial and temporal scales, forming stress gradients. Multi-scale stress gradients influence ecosystem properties from niche characteristics and species distributions (e.g. Carboni et al., 2016), interactions between species (Bertness & Callaway, 1994; Bruno et al., 2003), to large-scale productivity patterns (Bai et al., 2008; Zhao & Running, 2010). Stress gradients can also influence emergent ecosystem properties, including ecosystem resistance to and recovery from disturbance (Capdevila et al., 2019; van Belzen et al., 2017). The ability of communities to resist and recover from disturbance is a crucial part of ecosystem resilience (Gunderson, 2000; Holling, 1973, 1996). Resilience is a foundational concept in ecology (Holling, 1973; Standish et al., 2014) and has been contentiously defined over the years (Grimm & Wissel, 1997). Here, we use resilience as a general term encompassing several related concepts: the ability of an ecosystem to recover after disturbance to reference levels of some function (hereafter recovery or recovery status), the rate of that recovery (Holling, 1996; hereafter recovery rate) and the ability of an ecosystem to resist transitioning to an alternative state after disturbance (Holling, 1973; hereafter resistance).

The menagerie of terms describing ecosystem response to disturbance has been conceptualized in a simplified and useful heuristic, the ball-and-cup model (Beisner et al., 2003). In this model, community states are represented by the ball, and the 'landscape' of all possible states is represented by the cup (Figure 1). Disturbances move the ball in a direction on the 'landscape' while changes in environmental conditions can change the 'landscape' itself (and indirectly, the ball; Beisner et al., 2003). If a disturbance is severe enough, or the 'landscape' is changed enough, a community can transition to an alternative state (Figure 1). Although this model has provided a useful conceptual baseline for theorizing how ecosystem resilience responds to environmental stress gradients or population changes, quantifying the component pieces of the model is not straightforward. This is problematic, as quantifying the relationships between stress gradients and ecosystem response to disturbance is crucial for scaling up experimental and plot-scale work. There is still disagreement regarding how best to tackle the problem of quantifying resilience (see Angeler & Allen, 2016 and articles cited within). Additionally, as single metrics or responses are often used in disturbance recovery work, it is difficult to decide which responses should be measured as legitimate proxies for the emergent and multivariate properties that allow ecosystems to resist and recover from disturbances.

Recent advances in predicting ecosystem response to disturbance have been made by rigorously quantifying ecosystem properties like recovery and resistance in a multivariate framework, combining several response variables into one metric. Baho et al. (2017), for example, parse resilience into constituent parts to operationalize and objectively quantify resilience, presenting a coherent set of hypotheses to test in ecosystems. Multivariate approaches are also being used to investigate resilience and other complex ecosystem responses in novel ways (Barros et al., 2016; Blonder, 2017; Lamothe et al., 2017, 2019), with both simulated and field data (e.g. Hillebrand et al., 2018). These multivariate methods hold promise for exploring resilience at landscape-relevant scales (Cushman & McGarigal, 2019) and lay out a consistent and rigorous framework for quantifying resilience concepts (e.g. the ball-and-cup model; Figure 1) that more accurately represent community- or ecosystem-level responses.

The influence of environmental stress gradients on ecosystem properties like recovery and resistance is especially relevant as climate change is shifting abiotic baselines, potentially moving ecosystems towards more stressful conditions (IPCC, 2013). Experiments are already being used to explore how changing environmental gradients influence resilience, for example, showing that univariate resilience decreases (critical slowing down) as stresses such as flooding increase (van Belzen et al., 2017). Pinpointing environmental drivers and underlying mechanisms that control ecosystem response to disturbance is needed to predict shifts in ecosystem response to chronic climate change stressors, especially as pulse events interact with changing baseline conditions to influence ecosystem function (Harris et al., 2018). Mapping resilience along stress gradients will additionally allow the quantification of both imperiled and resilient patches of habitat at several spatial scales, giving managers and restoration practitioners spatially explicit guidance on ecosystem management options before state changes occur. Beyond management implications, resilience may exhibit spatial clustering or patterns at specific scales (Karatayev & Baskett, 2020) that can provide greater mechanistic insight, but may not be obvious from patch-level analyses or experimental plots (Coop et al., 2019; Falk et al., 2019).

Salt marshes are excellent study systems to explore how ecosystem resilience may be influenced by environmental stress gradients, as they are located naturally along flooding gradients that are well characterized (Adam, 1993; Mitsch & Gosselink, 2007). These ecosystems are also typically dominated by only a few herbaceous plant species, making the measurement and disentanglement of community responses to disturbance more viable within years, not decades. Furthermore, salt marshes are actively transitioning to unvegetated mudflats as flooding tolerance is exceeded from sea-level rise, illustrating two distinct states (e.g. Wang & Temmerman, 2013). The transition from vegetated to unvegetated states can occur from flooding alone, or from natural disturbances to vegetated patches (Kirwan & Murray, 2007) such as temporary wrack deposition (e.g. Reidenbaugh

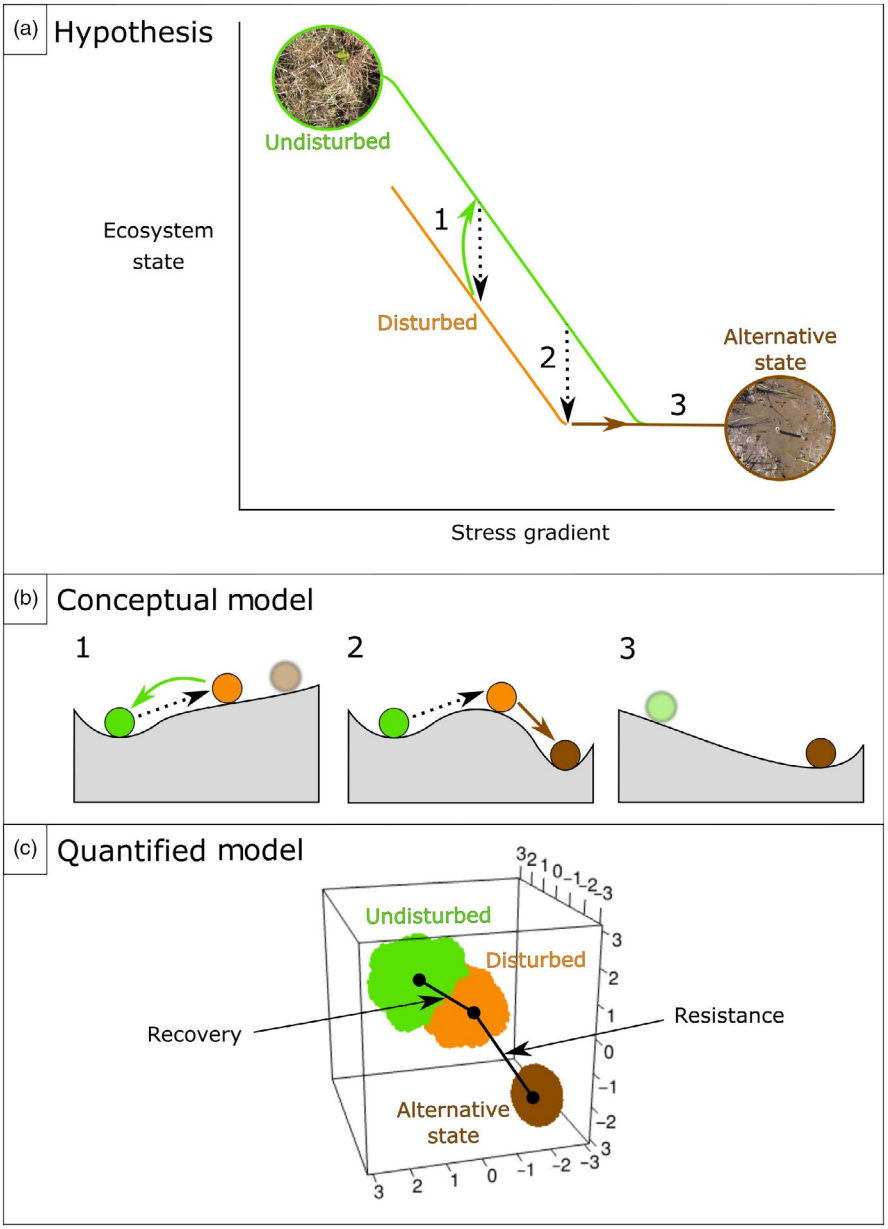

FIGURE 1 (a) Hypothesis, (b) conceptual model and (c) quantified model. (a) Hypothesis: in a system with two states (e.g. salt marsh and mudflat), increasing stress along a gradient linearly degrades the system. When episodic disturbance is included in combination with chronic stress, the system is perturbed but recovers (1) or a threshold emerges that can transition the system into an unvegetated state (2). Past a certain chronic stress value, the system transitions into an unvegetated state without disturbance (3). (b) Conceptual model: ball-and-cup conceptual model of state change for (1) system along the less stressful portion of the gradient. Disturbance perturbs the system but it returns to a vegetated state and there is effectively one possible ecosystem state; the unvegetated state is not stable. (2) A system along the portion of the gradient where alternative states exist. Without disturbance, the system remains in the vegetated state, but with disturbance the system transitions into the alternative, unvegetated state. (3) A system along the most stressful portion of the gradient. Emergent vegetation cannot survive so there is effectively one ecosystem state; the vegetated state is not stable. (c) Quantified model: using a hypervolume framework, we quantify the conceptual ball-and-cup model and measure resilience metrics at time t_{0+n} after disturbance. Recovery is the centroid distance between undisturbed and disturbed hypervolumes, and resistance is the centroid distance between disturbed and the alternate, unvegetated state hypervolume

& Banta, 1980). Finally, salt marshes are the target of restoration activities seeking to increase elevation to buffer coastal wetlands against sea-level rise and flooding stress. Comparing restored salt marshes that are situated at higher elevations to natural marshes that are situated at lower elevations provides a broader range of hydrologic conditions to gain further insight to stress responses. Knowledge gained from salt marshes can inform how stress gradients influence resilience and stable state theory more broadly.

In this study, we quantified stress gradient control on multivariate plant community recovery status, recovery rate and resistance along a flooding stress gradient at natural and restored salt marshes in southeastern Louisiana, using a combination of disturbance-recovery experiments and *n*-dimensional hypervolume modelling (Figure 1). We further elucidated potential mechanistic drivers of multivariate recovery and resistance. Finally, we used a combination of ground- and airborne-based data to map multivariate recovery and the existence of alternative states at the landscape scale and quantified the resultant spatial patterns. Our objectives were to (a) quantify the conceptual ball-and-cup resilience model for a salt marsh system with an alternative mudflat state; (b) using the quantified ball-and-cup model, test how pre-disturbance abiotic stress influences post-disturbance plant community recovery and resistance, and what mechanisms may explain observed patterns; and (c) investigate spatial patterns of plant community resilience and alternative states at the landscape scale.

2 | MATERIALS AND METHODS

2.1 | Study sites and experimental design

We established plots in *Spartina alterniflora*-dominated salt marsh in southeastern Louisiana, USA (Figure S1). Saline marshes in

southeastern Louisiana are mineral dominated (21% organic matter, 0.38 g/cm^3 bulk density; Wang et al., 2017) and are situated on active or abandoned delta lobes of the Mississippi River. Through the interplay of organic production and mineral deposition, coastal wetlands dominated by *S. alterniflora* can keep pace with sea-level rise (Morris et al., 2002), although the staggering rates of relative sea-level rise locally (9.1 mm/year at Grand Isle; NOAA, 2020) combined with hydrologic and sediment alterations from human management decisions have led to high rates of regional marsh loss (e.g. Twilley et al., 2016). While the overall pattern of marsh loss is often attributed to increased flooding from sea-level rise, the proximate mechanisms that trigger marsh conversion to mudflat are still unclear.

We established plots at two natural marshes that serve as reference sites (29.1800°N, 90.2410°W; 29.1935°N, 90.2452°W) and two restored marshes (restored in 2002, 29.1843°N, 90.2383°W; restored in 2014, 29.1347°N, 90.2255°W). Both restored sites received sediment slurry amendments (Mendelssohn & Kuhn, 2003). At each natural and restored site, three replicate transects were established along elevation gradients from low to high elevation using real-time kinematic surveying in NAVD88 Geoid 12A (Trimble R-8 Receiver & TSC3 Controller; Trimble Inc.). Transects were established so that elevations overlapped between site types (natural 0.09 m–0.26 m NAVD88, restored 0.17 m–0.33 m NAVD88). The experimental design consisted of 45 total plots, with 18 natural site plots (9 per site) and 27 restored site plots (12 or 15 per site). All sites experienced diurnal micro-tides (0.37 m tide range; NOAA, 2017). To calculate percent inundation for each plot, we developed a relationship between elevation and water levels from the nearest surveyed Coastal Reference Monitoring System gage, which was less than 6 km from all sites and experienced similar hydrologic conditions (CRMS0292; CRMS, 2018). We calculated percent inundation in 5 cm increments (m NAVD88 GEOID12A) using 3 years of data. We then fit a polynomial model to the elevation–inundation relationship and extracted model parameters. Finally, we applied plot-specific elevation values (m NAVD88) to this relationship to derive percent inundation for each experimental plot individually.

At each plot, a PVC pole marked the centre of a 1 m^2 circle subplot (0.56 m radius). Subplots were experimentally disturbed in April 2016 by clipping and removing all above-ground vegetation to the soil surface, similar to non-lethal disturbances applied in Slocum and Mendelssohn (2008) and van Belzen et al. (2018). This disturbance mimicked wrack deposition, a common acute disturbance in these marshes that can top-kill patches of salt marsh vegetation on the order of square metres (Figure S2 and Video S1). As a reference comparison to disturbed subplots, an undisturbed plot was established at each elevation and site combination (15 total plots). All plots were then monitored over time for 12 months, until April 2017.

2.2 | Field data collection

To quantify above-ground plant community structure, stem density (live and dead) was recorded in 0.25 m × 0.25 m quadrats, percent cover was visually estimated for the entire 1 m^2 subplot and average plant height was measured for disturbed and undisturbed plots. Quadrats were placed at the plot centre in the same orientation during each site visit to allow repeated measurements of the same ground footprint. Sites were visited and sampled for structural data eight times within the first year after disturbance (at time of disturbance, 0.5, 1, 3, 5, 7, 10 and 12 months post-disturbance).

To quantify above-ground biomass responses, we harvested above-ground biomass in 0.25 m × 0.25 m quadrats in each disturbed and undisturbed subplot one year after disturbance. Tissue was put into coolers after harvest and taken to the laboratory where it was immediately frozen until processed. Above-ground tissue was separated into live and dead fractions and dried to constant mass at 65°C. Total stem density was quantified by summing the number of live and dead stems. To quantify below-ground biomass responses, we collected 10 cm diameter soil cores to a depth of 20 cm in each disturbed and undisturbed subplot one year after disturbance. Cores were placed into coolers after harvest and refrigerated in the laboratory at 4°C until processed. Cores were washed of all sediment over a 2-mm sieve and below-ground biomass was sorted into live root, live rhizome, dead root and dead rhizome fractions using flotation, colour and turgor as markers of live tissue (similar to Darby & Turner, 2008). Dead root and dead rhizome fractions were combined into one dead tissue fraction for analysis. Each below-ground biomass fraction was dried to constant mass at 65°C.

We also measured soil edaphic variables to characterize the overall soil environment, including indicators of stressful flooding conditions. Soil redox potential was recorded from two probes at each elevation at each site (15 samples of 2 probes per sample); probes were inserted to a depth of 10 cm and allowed to equilibrate to field conditions for at least 30 min before recording measurements (Patrick et al., 1996; Orion ORP Electrode 9179BN; Thermo Fisher Scientific Inc.). This measurement gave a snapshot of differences in soil redox conditions between sites and elevations (Stagg & Mendelssohn, 2010). Bulk density was also quantified using duplicate cores taken at each elevation at each site (15 samples of 2 cores per sample), using a weight to volume ratio (Blake & Hartge, 1986). Finally, soil porewater was sampled using sippers inserted to 10 cm; pH and conductivity (pH/CON 450 meter; Oakton Instruments) were measured in duplicate at each elevation at each site (15 duplicate samples), and NO_x and NH_4 concentrations were quantified in duplicate at a subset of elevations at each site (7 duplicate samples); nutrient samples were vacuum-filtered and sent to Louisiana State University for analysis.

2.3 | Data simulation and quantifying multivariate resilience

We used field-collected data to model plant community resilience in a multivariate framework, using R statistical software v3.4 and package 'HYPERVOLUME' (Figure 1; Blonder et al., 2018; R Core Team, 2016). Linear mixed models (package 'NLME' in R; Pinheiro et al., 2016) were

fit to collected data for undisturbed and disturbed marsh plots separately (Figures S3–S12; Model parameters in Tables S1 and S2). Disturbed model curves were not allowed to have higher response values than undisturbed model curves at a given value of *x* (see Figures S3–S12). This ensured differences between undisturbed and disturbed marsh model curves were due to lack of recovery, not overcompensation (e.g. McNaughton, 1983). We simulated plant biomass data for disturbed and undisturbed marsh plots along the elevation gradient using linear mixed model predictions. Biomass data were simulated for each response variable by generating 100 points for each predictor combination of interest, assuming normal distributions (as in James et al., 2020). For structural responses measured over time, data were additionally simulated for each time step of interest (every 30 days after initial disturbance for one year) by generating 50 points for each predictor combination.

n-dimensional hypervolumes for each combination of elevation, site and/or time were created using simulated data for disturbed and undisturbed marsh plots following recommendations of Blonder et al. (2018) and Barros et al. (2016; detailed in methods supplement). We combined single responses (chosen a priori) into hypervolumes representing disturbed and undisturbed marsh plant biomass one year after disturbance (responses in Tables S1 and S2). Additionally, hypervolumes representing the structure of disturbed and undisturbed marsh plant communities were created over time (responses in Tables S1 and S2). Finally, an alternative state hypervolume was created representing an unvegetated mudflat state that marshes may transition to given enough flooding stress and/or disturbance. This simulated mudflat state contained no live plant biomass above or below-ground but contained dead below-ground biomass (average values of field-collected data from live plots).

We compared hypervolumes using several multivariate metrics to quantify recovery, recovery rates and resistance of the simulated plant communities. To quantify recovery, we calculated centroid distance between undisturbed and disturbed marsh hypervolumes at each elevation and site combination; centroid distances closer to 0 represent higher recovery one year after disturbance. To quantify resistance to state change, we calculated centroid distance between disturbed marsh hypervolumes and the alternative state mudflat hypervolume at each elevation and site combination; centroid distances closer to 0 represent lower resistance to state change. Variation around centroid distances was quantified as the average distance between 1,000 hypervolumes generated using random assignment of data to groups (bootstrapping). Centroid distances were visualized along elevation and site gradients using loess smoothers; if centroid distance was within the bootstrapped variance around 0, marsh hypervolumes were considered fully recovered (for recovery) or to have transitioned into an alternative state (for resistance) one year after disturbance. To quantify recovery rates, we calculated centroid distances between disturbed and undisturbed marsh hypervolumes over time using community structure data for each combination of elevation and site type. To derive rate equations, we extracted parameters from curves fit using linear mixed models (all model parameters reported Tables S1 and S2).

2.4 | Drivers of resilience and spatial patterns

To explore potential drivers of recovery and resistance, we fit loess smoothers using a priori predictors (modelled soil conditions and field-collected undisturbed plot biomass) on recovery (multivariate centroid distance of simulated plant communities).

We used spatial datasets in combination with resilience metrics and elevation to map resilience onto the landscape. We started with the Estuarine and Marine Wetland class of wetland from the National Wetlands Inventory (NWI) for Louisiana (NWI, 2016). Estuarine and Marine Wetland polygons were clipped to the extent of the Louisiana Department of Wildlife and Fisheries coastal vegetation survey classified as Saline Vegetation (LDWF, 2013) using ArcGIS (Esri). Given the high rates of wetland loss in Louisiana, the NWI/LDWF coastal salt marsh polygons contained large areas of open water habitat. To remove open water, we leveraged Google Earth Engine and calculated normalized difference vegetation (NDVI) and water (NDWI) indices from 2015 National Agriculture Inventory Program (NAIP) imagery (USDA Farm Service Agency). We then generated a land/water classification map (2.5 m horizontal resolution) using the random forest algorithm and 400 haphazardly located training points. The final classification had a training accuracy of 96.9% and a Cohen's kappa of 0.94.

We used two LiDAR datasets (South Terrebonne, 2015 and Barataria, 2013 [nationalmap.gov]) to estimate coastal salt marsh platform elevation. We extracted minimum, mean and maximum elevation at 5 m resolution from the LAS files and calculated the vertical bias due to vegetation by differencing the minimum LiDAR elevation and CRMS survey-grade GPS elevation points. The elevation characteristics from the LiDAR and the 2015 NDVI from NAIP were used to calibrate a correction model that predicted vertical bias. This is similar to the LEAN technique from Buffington et al. (2016); however, we used a nonparametric boosted regression tree algorithm (package 'DISMO' in R; Hijmans et al., 2017) instead of multiple linear regression to correct the vertical bias. To convert elevations into percent inundation, we used CRMS water data from stations on the Terrebonne basin (CRMS0336; CRMS, 2018) and Barataria basin (CRMS0178; CRMS, 2018) sides of the Port Fourchon area; 3 years of data were analysed for relationships, including the year of field experiments and 2 years prior to experiments. Loggers were representative of the long-term mean sea level recorded by nearby CRMS gauges. Elevation and percent inundation were related in a linear model framework for each logger; we used these relationships to find the elevation that corresponded to each inundation transition in our resilience model.

After establishing inundation and elevation relationships for both Terrebonne and Barataria areas, we classified the corrected digital elevation model based on our resilience metrics; flooding levels above which our simulated communities transitioned to an alternative, unvegetated state one year after disturbance were considered imperiled (>52% inundated), and flooding levels below which our simulated plant communities transitioned to an alternative, unvegetated state one year after disturbance (i.e. levels where the marsh

showed recovery) were considered resilient (<52% inundated). For each basin, recovery was standardized so that full recovery (<15% inundated) was 1 and state change (>52% inundated) was 0; resilience was graphically represented along this standardized gradient. We excluded any locations that experienced more than 65% inundation as too low to support salt marsh vegetation (Snedden & Steyer, 2013; Stagg et al., 2020; 0.04 m NAVD88 Terrebonne area, 0.11 m NAVD88 Barataria area), and excluded any locations higher than 1.0 m NAVD88 as too high to support marsh vegetation (0% flooded in both cases). Finally, area of each resilience class was quantified for Terrebonne and Barataria areas, and for the Port Fourchon region as a whole using ArcGIS.

3 | RESULTS

3.1 | Recovery

Recovery of simulated plant communities was greater with decreased flooding and restoration one year after disturbance compared to natural marshes (Figure 2). Recovery was reduced with increasing flooding stress, with small differences between restored and unrestored sites (Figure 2). Simulated plant communities in disturbed plots generally did not recover to undisturbed levels within the study period; however, simulated communities flooded less than ~15% of the time fully recovered one year after disturbance (Figure 2). Lack of total recovery was primarily driven by a lack of above-ground dead tissue throughout all plots (Figure S4), with the most flooded treatments experiencing death of below-ground tissue and therefore no recovery during the study (Figures S6 and S7). All but the most flooded treatments exhibited positive recovery.

3.2 | Recovery rates

Recovery rates varied with both flooding stress and restoration activity for simulated plant communities (Figure 3; Table S3). Structural rates of recovery were nonlinear over time but did not follow the expected exponential function; instead, a quadratic function provided the best fit, mirroring seasonal changes in the marsh (turnover in dead stem density). Restoration activity increased the magnitude of both the linear and quadratic terms, increasing the initial rate of recovery and shifting maximum recovery earlier (Figure 3; Table S3). Flooding stress also slightly adjusted the linear term, but the linear term was primarily impacted by restoration activity (Table S3). Reduced flooding increased recovery rates in natural marshes, but not restored marshes (Figure 3). As the vertex of quadratic models was within the study time period, marshes were more recovered in winter 2017 (between 240 and 330 days) than at the end of the study period in April 2017 (365 days; Figure 3; Table S3). No communities fully recovered ecosystem structure during the study period, but all except the most flooded plots showed recovery.

3.3 | Resistance

Resistance of simulated plant communities was greater with decreased flooding stress and restoration one year after disturbance

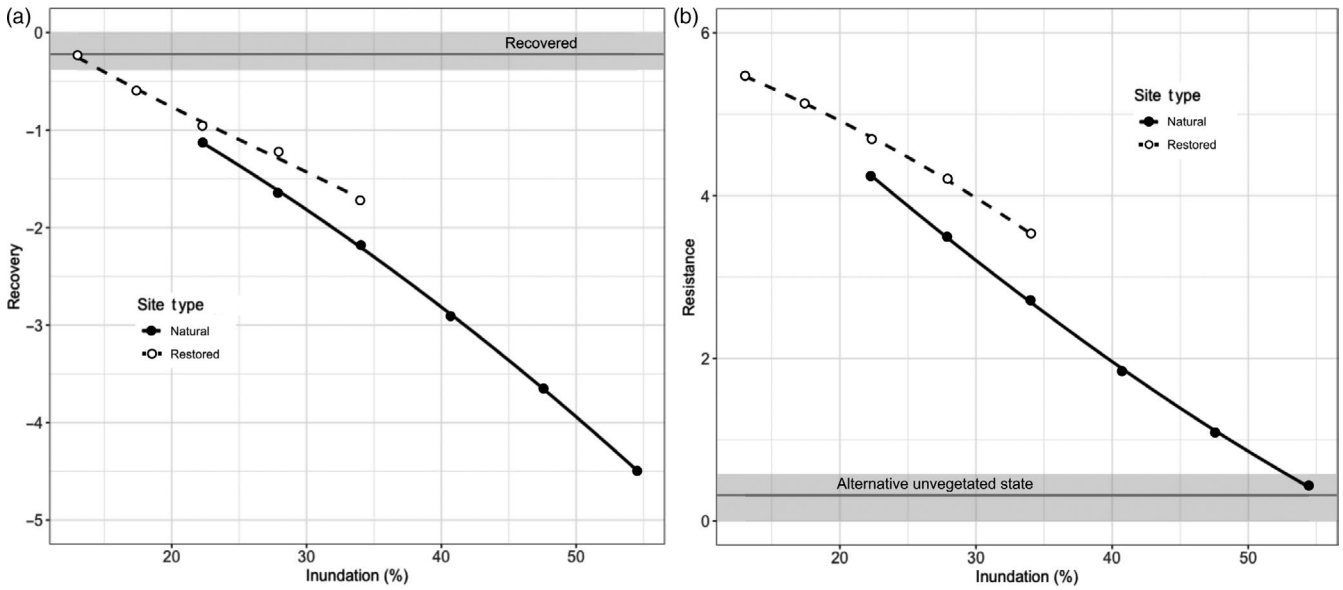

FIGURE 2 (a) Recovery and (b) resistance one year after disturbance along a flooding stress gradient at natural and restored sites as measured by centroid distance between (a) simulated disturbed and undisturbed communities or (b) simulated disturbed and the alternative, unvegetated state. Lines are loess smoothers for each site. Grey bands with solid grey lines represent 95% confidence intervals of the distance between bootstrapped communities; recovery values within the grey band represents sites that have fully recovered in panel (a) and resistance values within the grey band represent the transition to an alternative, unvegetated state in panel (b) one year after disturbance

(Figure 2). Resistance was steadily reduced with increasing flooding stress, with only small differences between restored and natural sites (Figure 2). Simulated plant communities generally exhibited resistance; however, simulated communities flooded more than ~52% of the time transitioned into an unvegetated state (Figure 2). This was due to death of below-ground tissue, evidenced by the lowest field plots containing no live below-ground (or therefore, above-ground) biomass one year after disturbance (Figures S3–S5). There was no evidence of clonal recolonization one year after disturbance.

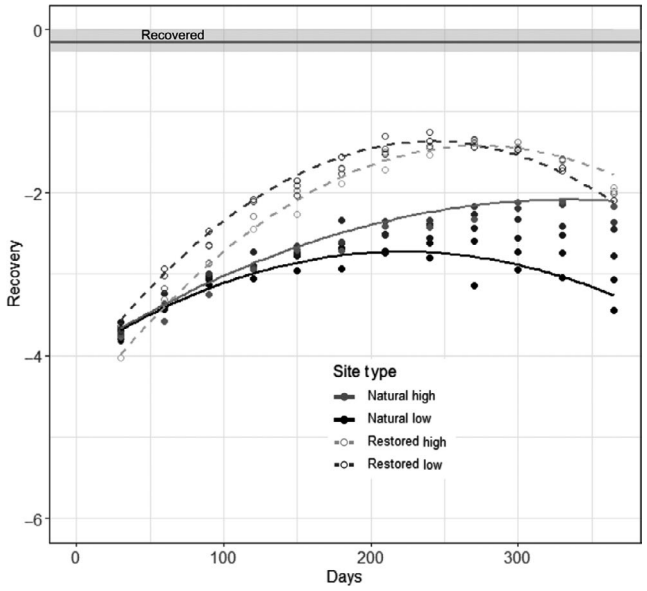

FIGURE 3 Rate of recovery of ecosystem structure at natural and restored salt marsh sites over time. Recovery measured by centroid distance between simulated disturbed and undisturbed communities. Lines are quadratic fits bounding the elevation gradients at each site. Grey band with solid black line represents 95% confidence interval of the distance between bootstrapped communities; recovery values within the grey band represent full recovery one year after disturbance

3.4 | Drivers of resilience

Simulated community recovery was greater with large modelled standing stocks of below-ground live root biomass in undisturbed plots (Figure 4a). Sites with undisturbed standing stocks above ~375 g/m^2 below-ground live root biomass fully recovered one year after disturbance. Below-ground biomass in salt marsh patches with low standing below-ground live biomass stocks did not survive the experimental disturbance. Sites with standing stocks below ~150 g/m^2 below-ground live root biomass transitioned into an unvegetated state after disturbance (Figure 4b). Modelled above-ground live biomass in undisturbed plots did not vary with hydrology, so was not related to recovery or resistance of simulated disturbed communities.

Soil conditions indicative of flooding stress were related, in turn, to standing stocks of below-ground live root biomass and therefore recovery (Figure S14). Higher soil bulk density values particularly occurred where greater below-ground live root biomass occurred (Figure S15). It is unclear whether the site type transition influenced the inflection point as a model artefact. Nevertheless, recovery decreased precipitously with bulk densities below ~0.25 g/cm^3. Other soil characteristics were highly variable and were not related to live root biomass standing stocks or recovery.

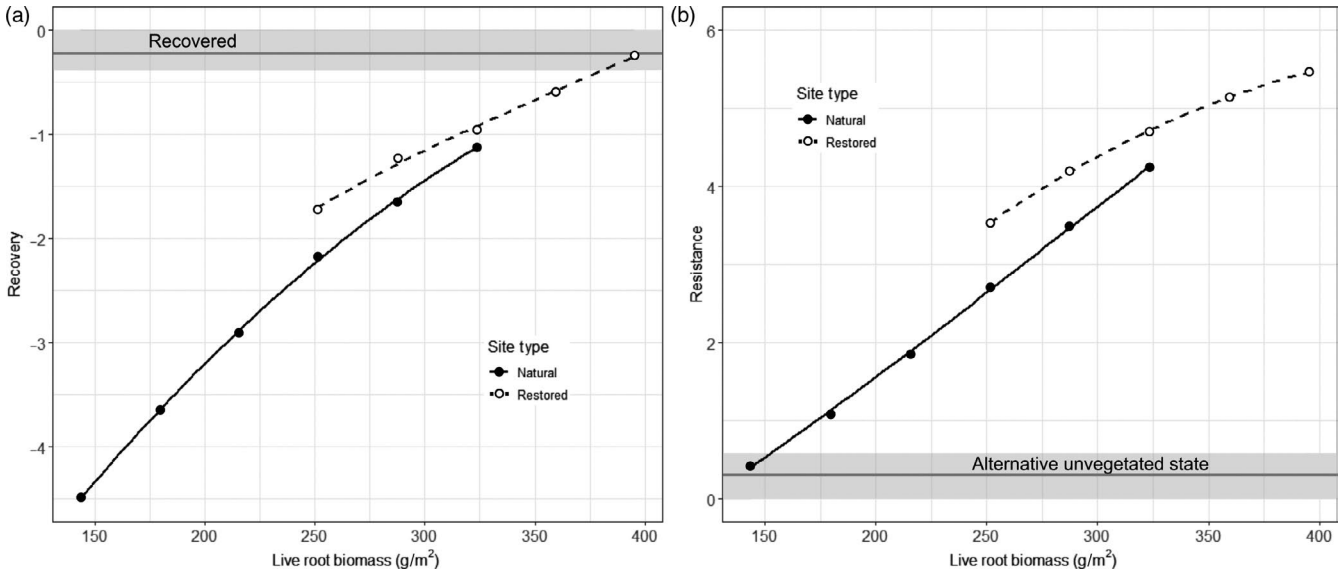

FIGURE 4 Relationship of modelled standing below-ground live biomass stocks in undisturbed communities and (a) recovery and (b) resistance one year after disturbance at natural and restored sites. Lines are loess smoothers for each site. Grey band with solid black line represents 95% confidence interval of the distance between bootstrapped communities; values within the grey band represent (a) full recovery and (b) transition to an alternative, unvegetated state

3.5 | Mapping resilience

Salt marsh in the Port Fourchon area was split almost evenly between imperiled marsh that is under such inundation stress that a single acute disturbance may transition it to mudflat (48%), and resilient marsh that recovers after a single acute disturbance (52%; Table 1; Figure 5). Terrebonne and Barataria areas within the broader region contained opposite patterns of spatial resilience; while 34% of salt marsh in the Terrebonne area was imperiled, twice that fraction, 67%, of the Barataria area was imperiled. As mean sea level for the Barataria area was higher than the Terrebonne area, this pattern may be caused by differences in water level, not marsh platform elevation. In total, more than 55 km^2 of salt marsh in the Port Fourchon area has the potential to transition to mudflat with acute disturbance events. Interior portions of marshes were lower and therefore less resilient to disturbance, while high creekbank marshes and restored sites exhibited the highest resilience across the landscape (Figure 5).

TABLE 1 Acreage of imperiled (>52% inundation) and resilient (<52% inundation) salt marsh for Terrebonne and Barataria areas, and the Port Fourchon region in southeastern Louisiana, USA. Percentages are taken as percent of each resilience class over total area in the sub-basin or region

Region	Imperiled marsh (km^2)	Resilient marsh (km^2)	Total marsh (km^2)
Terrebonne area	22.55 (34%)	43.39 (66%)	65.94
Barataria area	33.61 (67%)	16.93 (33%)	50.54
Port Fourchon region	56.16 (48%)	60.32 (52%)	116.48

4 | DISCUSSION

4.1 | Quantifying the conceptual ball-and-cup model

Our work adds to the growing literature quantifying the drivers of resilience, including recent work on the influence of connectivity (e.g. Shackelford et al., 2018; Standish et al., 2014), scale (e.g. Buma et al., 2019) and stress gradients (e.g. Cavanaugh et al., 2019; Lamothe et al., 2017). Multivariate work has further expanded understanding of resilience and stable state theory. Barros et al. (2016) provided one of the first examples of *n*-dimensional hypervolumes in a resilience context, investigating stability of simulated plant communities. While they did not explore resilience or alternative states explicitly, they laid the groundwork for hypervolumes to be used in that context. Lamothe et al. (2019) directly linked multivariate approaches (ordination) to the ball-and-cup analogy, providing an

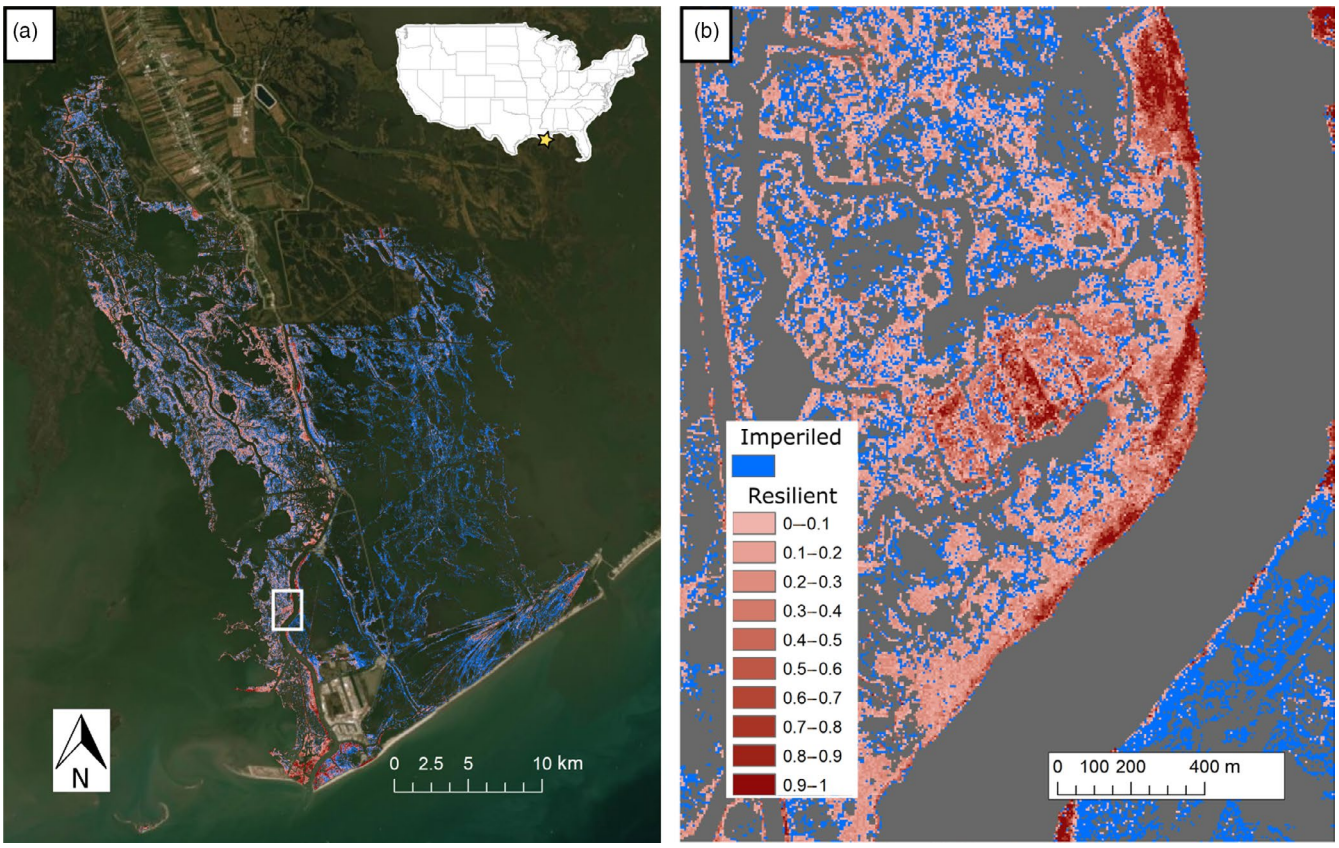

FIGURE 5 Resilience of salt marshes to disturbance in (a) Port Fourchon area, Louisiana, USA. (b) Inset of area around a restoration site (centred). Blue is imperiled habitat (transition to alternative, unvegetated state with acute disturbance), and red is resilient. The more intense red colour indicates higher resilience, up to a value of 1 which indicates full recovery within one year after disturbance

excellent example of using distance in ordination space to quantify resilience and other metrics by following communities through time. Here, we also use distance (in *n*-dimensional space) to quantify the ball-and-cup model, but have focused on differences between alternative states, and disturbed and undisturbed communities.

This approach can be extended as a comparable metric across ecosystems and scales. We use the plant component of an ecosystem, but any component or combination of components can be used to create a hypervolume of the system (e.g. quantifying resilience of soil nutrient cycling or the invertebrate community). Component members should be chosen a priori unless PCA or other ordination methods are used on large multivariate datasets to reduce dimensionality. For example, this method could be used to quantify alternative states along a forest aridity gradient and the resilience of plant biomass to forest fire disturbance (e.g. in the Southwest USA; Davis et al., 2019; Stevens-Rumann et al., 2018; Williams et al., 2010), albeit with a broader temporal window. All centroid distances are measured in standard deviations of *z*-scored variables, so the relative recovery and resistance in a forest/fire/aridity setting could potentially be compared to the current marsh/wrack/flooding setting. Additionally, varying intensities of disturbance could be used to determine if thresholds of state change differ by disturbance intensity. Much work remains to develop a coherent, quantified model of resilience and stable state theory that applies across scales and systems, but we believe *n*-dimensional hypervolumes hold promise.

4.2 | Resilience along a stress gradient

By quantifying the conceptual ball-and-cup model, we were able to quantify the interaction of an acute disturbance with an underlying stress gradient, and identify the range of conditions where alternative states are possible. Increasing stress reduced recovery and resistance. Others have used disturbance-recovery experiments along elevation gradients to explore univariate ecosystem resilience in salt marshes (Slocum & Mendelssohn, 2008; Stagg & Mendelssohn, 2011; van Belzen et al., 2017) and found that low elevation marshes in more stressful conditions are less resilient. In the present study, flooding stress reduced multivariate recovery up to the alternative, unvegetated state threshold. Recent work in congener *S. patens*, a high marsh species, found that decreasing elevation led to increasing fragmentation and depressed vegetation cover on the landscape (Stagg et al., 2020) or transition to low marsh (Gonneea et al., 2018). The transition where chronic flooding stress led to marked changes in vegetation cover occurred between 0.21 and 0.32 m MSL (Stagg et al., 2020); in the current study investigating more flood-tolerant *S. alterniflora*, chronic flooding stress influenced disturbance responses between −0.02 and 0.18 m MSL. While it is well established that increasing flooding stress from sea-level rise and reduced sediment delivery is driving conversion to mudflat and open water in certain coastal salt marsh settings (e.g. Couvillion et al., 2017), the proximate mechanisms causing conversion or specific tipping points require further study.

Our work supports the hypothesis that disturbance can interact with underlying pre-disturbance stress gradients to structure the spatial distribution of alternative states (e.g. Dantas et al., 2016 for tropical systems, Kirwan & Murray, 2007 for salt marshes). The chronic stress of flooding, like many stress gradients (Hillebrand et al., 2020), may not lead to threshold responses where state change occurs, instead following the pattern of linear degradation until vegetation can no longer survive. However, when disturbance is jointly considered, the interaction of increasing chronic stress and acute disturbance events can transition salt marsh to mudflat or open water, thereby creating a threshold response over some span of the stress gradient. In southeastern Louisiana, *S. alterniflora* marsh may not be able to survive more than ~65% inundation (Snedden & Steyer, 2013). In the current study, we identified a threshold inundation of 52% when disturbance mimicking natural wrack disturbance is considered. Therefore, between 52% and 65% inundation, we expect a threshold response and the existence of two alternative states in this system. The existence of two alternative states in marshes has been modelled in other regions (e.g. Wang & Temmerman, 2013), but is often made difficult by complex biogeomorphic feedbacks (Mariotti, 2020). Although wrack deposition or similar acute disturbances do not affect large contiguous swaths of salt marsh habitat at once, the combination of acute disturbance across the landscape with increasing flooding from sea-level rise may provide an additional mechanism for the widespread land loss observed in coastal Louisiana. With climate change increasing chronic stress gradients in many ecosystems (IPCC, 2013), understanding and modelling the interactions between shifting stress gradients and natural disturbance regimes is paramount, as the combination of press and pulse stressors can have synergistic effects (current study, Harris et al., 2018).

4.3 | Resilience mechanisms

We identified drivers of ecosystem recovery and resistance that may be crucial indicators of plant community resilience and alternative states more broadly. Ultimately, below-ground live biomass stocks predicted resistance and recovery after disturbance. Negative effects of flooding stress on plant survival are well characterized in salt marshes (Bradley & Morris, 1990; Mendelssohn & McKee, 1988). Increased flooding likely reduced resilience by limiting below-ground energy reserves and shifting relative energy allocation away from below-ground tissue (Mudd et al., 2009, but see Kirwan & Guntenspergen, 2015 for lack of response in non-*S. alterniflora* salt marsh). Few studies have looked at recovery of below-ground plant tissue to disturbance over time (but see Klopf et al., 2017). Interestingly, our findings corroborate earlier work in salt marshes suggesting that below-ground biomass is more responsive to environmental stressors (Crosby et al., 2017; Stagg et al., 2017) and provides an early indicator of deterioration (Turner et al., 2004). Turner et al. (2004) found that while aboveground biomass did not differ between healthy and impaired

marshes, below-ground biomass showed marked declines in impaired marshes, evidence of changing patterns of energy allocation away from below-ground tissue. The present study found the same general pattern; above-ground biomass was not predictive of resilience, but below-ground biomass was. Below-ground responses are therefore crucial as indicators of current system resilience to future disturbance in salt marshes, and perhaps herbaceous ecosystems more generally. Although multivariate approaches were necessary to quantify the ball-and-cup model and resilience metrics, univariate data are irreplaceable for mechanistic understanding of what is driving ecosystem responses.

We propose that below-ground live biomass should thus be prioritized in monitoring programs, as it is a sensitive indicator of resilience. This is especially crucial in coastal wetland ecosystems, as below-ground biomass responses can impact biogeomorphic feedbacks, whereby marshes can keep pace with increasing sea levels (Morris et al., 2002). If below-ground biomass perishes due to disturbance, mineralization of that biomass will cause elevation loss, which, in turn, further increases flooding stress, making recolonization unlikely. With non-lethal above-ground disturbance, the marsh additionally loses the ability to trap sediment using the friction provided by vegetation (Mudd et al., 2004). *S. alterniflora* can invade less than ideal patches using clonal connections (Pennings & Callaway, 2000), but with above- and below-ground biogeomorphic feedbacks interrupted in low-elevation patches where vegetation communities are at the boundary of flooding tolerance, we believe it is unlikely that recolonization is possible. Longer-term monitoring, however, is required to determine if the low-marsh transition to mudflat is permanent or if clonal recolonization occurs. The generality of relationships between below-ground biomass and resilience requires additional work in other systems.

4.4 | Mapping resilience

By working along stress gradients, we were able to map resilience and where alternative states may exist at broad landscape scales, but at a resolution that allows the investigation of local- and patch-scale spatial patterns. We found distinct spatial patterns of resilience at several scales. At the patch scale, low interior marshes and interior pond edges are likely to exhibit state change after disturbance; this matches previous work showing pond expansion and marsh dieback in interior, low areas in regions not directly exposed to wave action (McKee et al., 2004; Turner & Rao, 1990). At the landscape scale, western Barataria salt marshes in the region are more likely to exhibit state change than eastern Terrebonne salt marshes, which may explain why that region of Louisiana is experiencing such high rates of land loss and fragmentation (Couvillion et al., 2017). The Terrebonne area of Port Fourchon experiences lower average sea levels than the Barataria area but marsh platform elevations may be similar, although more intensive elevation and water surveys are needed to confirm this pattern. One drawback to applying resilience to the landscape is the dependence on good quality stress gradient information. Improving estimates of regional hydrologic regimes, for example by interpolating many water level gages for a region, should allow verification of the current pattern and expansion across saline marsh in southeastern Louisiana.

Spatially explicit quantification of resilience allows managers and policymakers to identify areas of habitat at high risk of conversion, informing decisions to restore or conserve habitat at regional and landscape scales (e.g. Chambers et al., 2019). This spatial resilience dataset provides a baseline for sea-level rise and climate scenario modelling to project how resilience across the landscape will change with shifting flooding frequency and duration, applying the state change thresholds identified here to sea-level rise model projections (e.g. Swanson et al., 2014 for the Pacific USA), for example, could provide estimates of resilience into the future. Furthermore, by explicitly mapping where alternative states may exist across the landscape in response to natural disturbance regimes (in this case wrack deposition, Tolley & Christian, 1999), investigations into the scale and clustering of alternative states become possible. If resilience to specific disturbances is strongly controlled by quantifiable stress gradients in other systems, mapping resilience and alternative states in a spatially explicit framework may be possible across ecosystems.

5 | CONCLUSIONS

Our approach coupling field experiments with simulations and *n*-dimensional hypervolume modelling quantified multivariate resilience of plant communities, an advance over single metric responses. This holistic framework allowed quantification of the ball and cup ('landscape') for a model salt marsh system (Beisner et al., 2003), and a more explicit quantification of transitions between alternative states (May, 1977; Scheffer et al., 2001). Recovery and resistance along the dominant stress gradient followed predictable patterns with below-ground plant biomass likely mechanistically driving responses. The strong relationship between underlying stress gradients and resilience properties allowed us to map resilience and alternative state existence onto the landscape, highlighting both widespread lack of resilience in coastal salt marsh, and pinpointing local landscape settings where salt marsh is most likely to transition into an alternative, unvegetated state after disturbance. Spatial mapping of resilience, as demonstrated here, opens up new possibilities for prediction and management of ecosystems in the face of disturbance and shifting baseline conditions, and allows previously unseen spatial patterns of resilience to emerge.

ACKNOWLEDGEMENTS

We would like to thank members of the Coastal Plant Ecology (J. Willis, M. McCoy) and Nelson Ecosystem Laboratory (C. Laurenzano, J. Lesser, J. Nelson) groups at the University of Louisiana at Lafayette, as well as O. Chapman, B. Miller and S. Short for field and laboratory assistance. B. Chiviou and C. Hall at the U.S. Geological Survey (USGS) Wetland and Aquatic Research Centre assisted in interpreting RTK elevation data. We thank L. Windham-Meyers (USGS), C. Angelini and two anonymous reviewers for their

insight and comments that greatly improved the manuscript. This research was partially funded by grants to S.F.J. from the Ecology Centre at ULL, the Graduate Student Organization at ULL and the Society of Wetland Scientists. Support for C.L.S. in part from U.S. Geological Survey Ecosystems program and South Central Climate Adaptation Science Center. Any use of trade, product or firm names is for descriptive purposes only and does not imply endorsement by the U.S. Government.

AUTHORS' CONTRIBUTIONS

S.F.J., C.L.S. and M.W.H. designed the study; S.F.J., E.S.Y., W.R.J. and C.L.S. collected resilience data in the field; S.F.J. and K.J.B. analysed the data with input from W.R.J.; S.F.J. led the writing of the manuscript. All authors contributed substantially to drafts and gave final approval for publication.

PEER REVIEW

The peer review history for this article is available at https://publons.com/publon/10.1111/1365-2745.13552.

DATA AVAILABILITY STATEMENT

Data available from Jones et al. (2020) (https://doi.org/10.5066/P9FNH7F6).

ORCID

Scott F. Jones https://orcid.org/0000-0002-1056-3785
Camille L. Stagg https://orcid.org/0000-0002-1125-7253
Erik S. Yando https://orcid.org/0000-0002-8786-6178
W. Ryan James https://orcid.org/0000-0002-4829-7742
Kevin J. Buffington https://orcid.org/0000-0001-9741-1241

REFERENCES

Adam, P. (1993). *Saltmarsh ecology*. Cambridge University Press.

Angeler, D. G., & Allen, C. R. (2016). Quantifying resilience. *Journal of Applied Ecology*, *53*, 617–624. https://doi.org/10.1111/1365-2664.12649

Baho, D. L., Allen, C. R., Garmestani, A., Fried-Petersen, H., Renes, S. E., Gunderson, L., & Angeler, D. G. (2017). A quantitative framework for assessing ecological resilience. *Ecology and Society*, *22*(3), 1–17. https://doi.org/10.5751/ES-09427-220317

Bai, Y., Wu, J., Xing, Q. I., Pan, Q., Huang, J., Yang, D., & Han, X. (2008). Primary production and rain use efficiency across a precipitation gradient on the Mongolia Plateau. *Ecology*, *89*(8), 2140–2153. https://doi.org/10.1890/07-0992.1

Barros, C., Thuiller, W., Georges, D., Boulangeat, I., & Münkemüller, T. (2016). N-dimensional hypervolumes to study stability of complex ecosystems. *Ecology Letters*, *19*, 729–742.

Beisner, B. E., Haydon, D. T., & Cuddington, K. (2003). Alternative stable states in ecology. *Frontiers in Ecology and the Environment*, *1*, 376–382.

Bertness, M. D., & Callaway, R. (1994). Positive interactions in communities: A post cold war perspective. *Trends in Ecology & Evolution*, *9*, 191–193. https://doi.org/10.1016/0169-5347(94)90088-4

Blake, G., & Hartge, K. (1986). Bulk Density. In A. Klute (Ed.), *Methods of soil analysis: Part 1 – Physical and mineralogical methods* (pp. 377–382). American Society of Agronomy.

Blonder, B. (2017). Hypervolume concepts in niche-and trait-based ecology. *Ecography*. *41*(9), 1441–1455.

Blonder, B., Morrow, C. B., Maitner, B., Harris, D. J., Lamanna, C., Violle, C., Enquist, B. J., & Kerkhoff, A. J. (2018). New approaches for delineating *n*-dimensional hypervolumes. *Methods in Ecology and Evolution*. *9*(2), 305–319.

Bradley, P. M., & Morris, J. T. (1990). Influence of oxygen and sulfide concentration on nitrogen uptake kinetics in *Spartina alterniflora*. *Ecology*, *71*, 282–287. https://doi.org/10.2307/1940267

Bruno, J. F., Stachowicz, J. J., & Bertness, M. D. (2003). Inclusion of facilitation into ecological theory. *Trends in Ecology & Evolution*, *18*, 119–125. https://doi.org/10.1016/S0169-5347(02)00045-9

Buffington, K. J., Dugger, B. D., Thorne, K. M., & Takekawa, J. Y. (2016). Statistical correction of lidar-derived digital elevation models with multispectral airborne imagery in tidal marshes. *Remote Sensing of Environment*, *186*, 616–625.

Buma, B., Harvey, B. J., Gavin, D. G., Kelly, R., Loboda, T., McNeil, B. E., Marlon, J. R., Meddens, A. J. H., Morris, J. L., Raffa, K. F., Shuman, B., Smithwick, E. A. H., & McLauchlan, K. K. (2019). The value of linking paleoecological and neoecological perspectives to understand spatially-explicit ecosystem resilience. *Landscape Ecology*, *34*, 17–33.

Capdevila, P., Hereu, B., Salguero-Gómez, R., Rovira, G., Medrano, A., Cebrian, E., Garrabou, J., Kersting, D. K., & Linares, C. (2019). Warming impacts on early life stages increase the vulnerability and delay the population recovery of a long-lived habitat-forming macroalga. *Journal of Ecology*, *107*(3), 1129–1140. https://doi.org/10.1111/1365-2745.13090

Carboni, M., Zelený, D., & Acosta, A. T. R. (2016). Measuring ecological specialization along a natural stress gradient using a set of complementary niche breadth indices. *Journal of Vegetation Science*, *27*(5), 892–903. https://doi.org/10.1111/jvs.12413

Cavanaugh, K. C., Reed, D. C., Bell, T. W., Castorani, M. C. N., & Beas-Luna, R. (2019). Spatial variability in the resistance and resilience of giant kelp in Southern and Baja California to a multiyear heatwave. *Frontiers in Marine Science*, *6*, 413.

Chambers, J. C., Brooks, M. L., Germino, M. J., Maestas, J. D., Board, D. I., Jones, M. O., & Allred, B. W. (2019). Operationalizing resilience and resistance concepts to address invasive grass-fire cycles. *Frontiers in Ecology and Evolution*, *7*, 185.

Coop, J. D., DeLory, T. J., Downing, W. M., Haire, S. L., Krawchuk, M. A., Miller, C., Parisien, M.-A., & Walker, R. B. (2019). Contributions of fire refugia to resilient ponderosa pine and dry mixed-conifer forest landscapes. *Ecosphere*, *10*(7), e02809. https://doi.org/10.1002/ecs2.2809

Couvillion, B., Beck, H., Schoolmaster, D., & Fischer, M. (2017). *Land area change in coastal Louisiana 1932 to 2016*. U. S. Geological Survey Scientific Investigations Map.

CRMS – Coastwide Reference Monitoring System. (2018). *Hourly hydrographic data for station numbers: 0178, 0292, 0336*. Retrieved from cims.coastal.louisiana.gov/DataDownload/DataDownload.aspx?type=hydro_hourly

Crosby, S. C., Angermeyer, A., Adler, J. M., Bertness, M. D., Deegan, L. A., Sibinga, N., & Leslie, H. M. (2017). *Spartina alterniflora* biomass allocation and temperature: Implications for salt marsh persistence with sea-level rise. *Estuaries and Coasts*, *40*(1), 213–223.

Cushman, S. A., & McGarigal, K. (2019). Metrics and models for quantifying ecological resilience at landscape scales. *Frontiers in Ecology and Evolution*, *7*, article 440.

Dantas, V. L., Hirota, M., Oliviera, R. S., & Pausas, J. G. (2016). Disturbance maintains alternative biome states. *Ecology Letters*, *19*, 12–19.

Darby, F. A., & Turner, R. E. (2008). Below- and aboveground *Spartina alterniflora* production in a Louisiana salt marsh. *Estuaries and Coasts*, *31*(1), 223–231.

Davis, K. T., Dobrowski, S. Z., Higuera, P. E., Holden, Z. A., Veblen, T. T., Rother, M. T., Parks, S. A., Sala, A., & Maneta, M. P. (2019). Wildfires and climate change push low-elevation forests across a critical climate threshold for tree regeneration. *Proceedings of*

the National Academy of Sciences of the United States of America, *116*(13), 6193–6198.

Falk, D. A., Watts, A. C., & Thode, A. E. (2019). Scaling ecological resilience. *Frontiers in Ecology and Evolution*, *7*, 275.

Gonneea, M. E., Maio, C. V., Kroeger, K. D., Hawkes, A. D., Mora, J., Sullivan, R., Madsen, S., Buzard, R. M., Cahill, N., & Donnelly, J. P. (2018). Salt marsh ecosystem restructuring enhances elevation resilience and carbon storage during accelerating relative sea-level rise. *Estuarine, Coastal and Shelf Science*, *217*, 56–68.

Grimm, V., & Wissel, C. (1997). Babel, or the ecological stability discussions: An inventory and analysis of terminology and a guide for avoiding confusion. *Oecologia*, *109*, 323–334. https://doi.org/10.1007/s004420050090

Gunderson, L. H. (2000). Ecological resilience-in theory and application. *Annual Review of Ecology and Systematics*, *31*, 425–439. https://doi.org/10.1146/annurev.ecolsys.31.1.425

Harris, R. M. B., Beaumont, L. J., Vance, T. R., Tozer, C. R., Remenyi, T. A., Perkins-Kirkpatrick, S. E., Mitchell, P. J., Nicotra, A. B., McGregor, S., Andrew, N. R., Letnic, M., Kearney, M. R., Wernberg, T., Hutley, L. B., Chambers, L. E., Fletcher, M.-S., Keatley, M. R., Woodward, C. A., Williamson, G., … Bowman, D. M. J. S. (2018). Biological responses to the press and pulse of climate trends and extreme events. *Nature Climate Change*, *8*, 579–587. https://doi.org/10.1038/s41558-018-0187-9

Hijmans, R. J., Phillips, S., Leathwick, J., & Elith, J. (2017). *dismo: species distribution modeling*. R package version 1.1-4.

Hillebrand, H., Donohue, I., Harpole, W. S., Hodapp, D., Kucera, M., Lewandowska, A. M., Merder, J., Montoya, J. M., & Freund, J. A. (2020). Thresholds for ecological responses to global change do not emerge from empirical data. *Nature Ecology & Evolution*, *4*, 1502–1509.

Hillebrand, H., Langenheder, S., Lebret, K., Lindström, E., Östman, Ö., & Striebel, M. (2018). Decomposing multiple dimensions of stability in global change experiments. *Ecology Letters*, *21*, 21–30. https://doi.org/10.1111/ele.12867

Holling, C. S. (1973). Resilience and stability of ecological systems. *Annual Review of Ecology and Systematics*, *4*(1), 1–23. https://doi.org/10.1146/annurev.es.04.110173.000245

Holling, C. S. (1996). *Engineering within ecological constraints*. National Academy.

IPCC. (2013). *Climate change 2013: The physical science basis. Contribution of working group I to the fifth assessment report of the intergovernmental panel on climate change*. Cambridge University Press.

James, W. R., Lesser, J. S., Litvin, S. Y., & Nelson, J. A. (2020). Assessment of food web recovery following restoration using resource niche metrics. *Science of the Total Environment*, *711*, 134801. https://doi.org/10.1016/j.scitotenv.2019.134801

Jones, S. F., Stagg, C. L., Yando, E. S., James, W. R., Buffington, K. J., & Hester, M. W. (2020). *Field and simulated data to construct hypervolumes of coastal wetland plant states for resilience quantification, Louisiana, USA (2016–2017)*. U.S. Geological Survey data release. https://doi.org/10.5066/P9FNH7F6

Karatayev, V. A., & Baskett, M. L. (2020). At what spatial scales are alternative stable states relevant in highly interconnected ecosystems? *Ecology*, *101*(2), e02930. https://doi.org/10.1002/ecy.2930

Kirwan, M. L., & Guntenspergen, G. R. (2015). Response of plant productivity to experimental flooding in a stable and submerging marsh. *Ecosystems*, *18*, 903–913.

Kirwan, M. L., & Murray, A. B. (2007). A coupled geomorphic and ecological model of tidal marsh evolution. *Proceedings of the National Academy of Sciences of the United States of America*, *104*(15), 6118–6122.

Klopf, R. P., Baer, S. G., Bach, E. M., & Six, J. (2017). Restoration and management for plant diversity enhances the rate of belowground ecosystem recovery. *Ecological Applications*, *27*, 355–362. https://doi.org/10.1002/eap.1503

Lamothe, K. A., Jackson, D. A., & Somers, K. M. (2017). Utilizing gradient simulations for quantifying community-level resistance and resilience. *Ecosphere*, *8*, e01953. https://doi.org/10.1002/ecs2.1953

Lamothe, K. A., Somers, K. M., & Jackson, D. A. (2019). Linking the ball-and-cup analogy and ordination trajectories to describe ecosystem stability, resistance, and resilience. *Ecosphere*, *10*(3), e02629.

LDWF. (2013). *Louisiana coastal marsh vegetative type map*. Louisiana Department of Wildlife and Fisheries, LSU AgCenter, and U.S. Geological Survey Wetland and Aquatic Research Center.

Mariotti, G. (2020). Beyond marsh drowning: The many faces of marsh loss (and gain). *Advances in Water Resources*, *144*, 103710.

May, R. M. (1977). Thresholds and breakpoints in ecosystems with a multiplicity of stable states. *Nature*, *269*, 471–477. https://doi.org/10.1038/269471a0

McKee, K., Mendelssohn, I., & Materne, M. (2004). Acute salt marsh die-back in the Mississippi River deltaic plain: A drought-induced phenomenon? *Global Ecology and Biogeography*, *13*(1), 65–73. https://doi.org/10.1111/j.1466-882X.2004.00075.x

McNaughton, S. J. (1983). Compensatory plant growth as a response to herbivory. *Oikos*, *40*, 329–336. https://doi.org/10.2307/3544305

Mendelssohn, I. A., & Kuhn, N. L. (2003). Sediment subsidy: Effects on soil-plant responses in a rapidly submerging coastal salt marsh. *Ecological Engineering*, *21*, 115–128. https://doi.org/10.1016/j.ecoleng.2003.09.006

Mendelssohn, I. A., & McKee, K. L. (1988). Spartina alterniflora die-back in Louisiana: Time-course investigation of soil waterlogging effects. *Journal of Ecology*, *76*(2), 509–521. https://doi.org/10.2307/2260609

Mitsch, W. J., & Gosselink, J. G. (2007). *Wetlands*. John Wiley and Sons.

Morris, J. T., Sundareshwar, P. V., Nietch, C. T., Kjerfve, B., & Cahoon, D. R. (2002). Responses of coastal wetlands to rising sea level. *Ecology*, *83*(10), 2869–2877.

Mudd, S. M., Fagherazzi, S., Morris, J. T., & Furbish, D. J. (2004). Flow, sedimentation, and biomass production on a vegetated salt marsh in South Carolina: toward a predictive model of marsh morphologic and ecologic evolution. In S. Fagherazzi, M. Marani, & L. K. Blum (Eds.), *The ecogeomorphology of tidal marshes*. Coastal and estuarine studies (Vol. *59*, pp. 165–187). American Geophysical Union.

Mudd, S. M., Howell, S. M., & Morris, J. T. (2009). Impact of dynamic feedbacks between sedimentation, sea-level rise, and biomass production on near-surface marsh stratigraphy and carbon accumulation. *Estuarine, Coastal and Shelf Science*, *82*(3), 377–389.

National Wetlands Inventory. (2016). *National Wetland Inventory – Version 2 – Surface Waters and Wetlands Inventory*. US Fish and Wildlife Service. Retrieved from https://www.fws.gov/wetlands/Data/Mapper.html

NOAA. (2017). *NOAA Tides & Currents – Station Info. for Port Fourchon, Belle Pass, LA – Station ID: 8762075*. Retrieved from https://tidesandcurrents.noaa.gov/stationhome.html?id=8762075

NOAA. (2020). NOAA Tides & Currents - Station Info. for Grand Isle, LA - Station ID: 8761724. Retrieved from https://tidesandcurrents.noaa.gov/stationhome.html?id=8762075

Patrick, W. H., Gambrell, R. P., & Faulkner, S. P. (1996). Redox measurements of soils. In: *Methods of soil analysis. Part 3. Chemical methods*. SSSA Book Series no. 5 (pp. 1255–1273). Soil Science Society of America and American Society of Agronomy.

Pennings, S. C., & Callaway, R. M. (2000). The advantages of clonal integration under different ecological conditions: A community-wide test. *Ecology*, *81*(3), 709–716.

Pinheiro, J., Bates, D., DebRoy, S., Sarkar, D. & R Core Team. (2016). nlme: Linear and nonlinear mixed effects models. https://cran.r-project.org/web/packages/nlme/index.html

R Core Team. (2016). *R: A language and environment for statistical computing*. R Foundation for Statistical Computing.

Reidenbaugh, T. G., & Banta, W. C. (1980). Origin and effects of *Spartina* wrack in a Virginia salt marsh. *Gulf Research Reports*, *6*(4), 393–401.

Scheffer, M., Carpenter, S., Foley, J. A., Folke, C., & Walker, B. (2001). Catastrophic shifts in ecosystems. *Nature*, *413*, 591. https://doi.org/10.1038/35098000

Shackelford, N., Standish, R. J., Lindo, Z., & Starzomski, B. M. (2018). The role of landscape connectivity in resistance, resilience, and recovery of multi-trophic microarthropod communities. *Ecology*, *99*(5), 1164–1172. https://doi.org/10.1002/ecy.2196

Slocum, M. G., & Mendelssohn, I. A. (2008). Use of experimental disturbances to assess resilience along a known stress gradient. *Ecological Indicators*, *8*, 181–190. https://doi.org/10.1016/j.ecolind.2007.01.011

Snedden, G. A., & Steyer, G. D. (2013). Predictive occurrence models for coastal wetland plant communities: Delineating hydrologic response surfaces with multinomial logistic regression. *Estuarine, Coastal and Shelf Science*, *118*(10), 11–23.

Stagg, C. L., & Mendelssohn, I. A. (2010). Restoring ecological function to a submerged salt marsh. *Restoration Ecology*, *18*(s1), 10–17. https://doi.org/10.1111/j.1526-100X.2010.00718.x

Stagg, C. L., & Mendelssohn, I. A. (2011). Controls on resilience and stability in a sediment-subsidized salt marsh. *Ecological Applications*, *21*, 1731–1744. https://doi.org/10.1890/09-2128.1

Stagg, C. L., Osland, M. J., Moon, J. A., Hall, C. T., Feher, L. C., Jones, W. R., Couvillion, B. R., Hartley, S. B., & Vervaeke, W. C. (2020). Quantifying hydrologic controls on local-and landscape-scale indicators of coastal wetland loss. *Annals of Botany*, *125*(2), 365–376.

Stagg, C. L., Schoolmaster, D. R., Piazza, S. C., Snedden, G., Steyer, G. D., Fischenich, C. J., & McComas, R. W. (2017). A landscape-scale assessment of above-and belowground primary production in coastal wetlands: Implications for climate change-induced community shifts. *Estuaries and Coasts*, *40*(3), 856–879.

Standish, R. J., Hobbs, R. J., Mayfield, M. M., Bestelmeyer, B. T., Suding, K. N., Battaglia, L. L., Eviner, V., Hawkes, C. V., Temperton, V. M., Cramer, V. A., Harris, J. A., Funk, J. L., & Thomas, P. A. (2014). Resilience in ecology: Abstraction, distraction, or where the action is? *Biological Conservation*, *177*, 43–51. https://doi.org/10.1016/j.biocon.2014.06.008

Stevens-Rumann, C. S., Kemp, K. B., Higuera, P. E., Harvey, B. J., Rother, M. T., Donato, D. C., Morgan, P., & Veblen, T. T. (2018). Evidence for declining forest resilience to wildfires under climate change. *Ecology Letters*, *21*(2), 243–252.

Swanson, K. M., Drexler, J. Z., Schoellhamer, D. H., Thorne, K. M., Casazza, M. L., Overton, C. T., Callaway, J. C., & Takekawa, J. Y. (2014). Wetland accretion rate model of ecosystem resilience (WARMER) and its application to habitat sustainability for endangered species in the San Francisco Estuary. *Estuaries and Coasts*, *37*(2), 476–492.

Tolley, P. M., & Christian, R. R. (1999). Effects of increased inundation and wrack deposition on a high salt marsh plant community. *Estuaries*, *22*, 944–954. https://doi.org/10.2307/1353074

Turner, R. E., & Rao, Y. S. (1990). Relationships between wetland fragmentation and recent hydrologic changes in a deltaic coast. *Estuaries*, *13*(3), 272–281. https://doi.org/10.2307/1351918

Turner, R. E., Swenson, E. M., Milan, C. S., Lee, J. M., & Oswald, T. A. (2004). Below-ground biomass in healthy and impaired salt marshes. *Ecological Research*, *19*(1), 29–35. https://doi.org/10.1111/j.1440-1703.2003.00610.x

Twilley, R. R., Bentley, S. J. Sr, Chen, Q., Edmonds, D. A., Hagen, S. C., Lam, N. S. N., Willson, C. S., Xu, K., Braud, D. W., Hampton Peele, R., & McCall, A. (2016). Co-evolution of wetland landscapes, flooding, and human settlement in the Mississippi River Delta Plain. *Sustainability Science*, *11*, 711–731.

van Belzen, J., van de Koppel, J., Kirwan, M. L., Guntenspergen, G. R., & Bouma T. J. (2017). Disturbance-recovery experiments to assess resilience of ecosystems along a stress gradient. *Protocol Exchange*, https://doi.org/10.1038/protex.2017.028

van Belzen, J., van de Koppel, J., Kirwan, M. L., van der Wal, D., Herman, P. M. J., Dakos, V., Kéfi, S., Scheffer, M., Guntenspergen, G. R., & Bouma, T. J. (2017). Vegetation recovery in tidal marshes reveals critical slowing down under increased inundation. *Nature Communications*, *8*, ncomms15811. https://doi.org/10.1038/ncomms15811

Wang, C., & Temmerman, S. (2013). Does biogeomorphic feedback lead to abrupt shifts between alternative landscape states?: An empirical study on intertidal flats and marshes. *Journal of Geophysical Research: Earth Surface*, *118*, 229–240.

Wang, H., Piazza, S. C., Sharp, L. A., Stagg, C. L., Couvillion, B. R., Steyer, G. D., & McGinnis, T. E. (2017). Determining the spatial variability of wetland soil bulk density, organic matter, and the conversion factor between organic matter and organic carbon across coastal Louisiana, U.S.A. *Journal of Coastal Research*, *33*(3), 507–517.

Williams, A. P., Allen, C. D., Millar, C. I., Swetnam, T. W., Michaelsen, J., Still, C. J., & Leavitt, S. W. (2010). Forest responses to increasing aridity and warmth in the southwestern United States. *Proceedings of the National Academy of Sciences of the United States of America*, *107*(50), 21289–21294.

Zhao, M., & Running, S. W. (2010). Drought-induced reduction in global terrestrial net primary production from 2000 through 2009. *Science*, *329*(5994), 940–943.

SUPPORTING INFORMATION

Additional supporting information may be found online in the Supporting Information section.

How to cite this article: Jones SF, Stagg CL, Yando ES, James WR, Buffington KJ, Hester MW. Stress gradients interact with disturbance to reveal alternative states in salt marsh: Multivariate resilience at the landscape scale. *J Ecol*. 2020;00:1–13. https://doi.org/10.1111/1365-2745.13552